Analytical Self-Consistent-Field Model of Weak Polyacid Brushes

Yu. V. Lyatskaya,[†] F. A. M. Leermakers,*[,‡] G. J. Fleer,[‡] E. B. Zhulina,[†] and T. M. Birshtein[†]

Department of Physical and Colloid Chemistry, Wageningen Agricultural University, Dreijenplein 6, 6703 HB, Wageningen, The Netherlands, and Institute of Macromolecular Compounds of Russian Academy of Science, St. Petersburg 199004, Russia

Received October 5, 1994; Revised Manuscript Received February 27, 1995[⊗]

ABSTRACT: An analytical self-consistent-field theory has been developed for a weak polyacid brush in which the degree of dissociation is controlled by the external pH of the solution. This theory gives analytical equations for the total brush thickness and for the root-mean-square (rms) thickness, the polymer profile, the end-point distribution function, and the local degree of dissociation of the brush molecules as a function of pH and the salt concentration. These results are in excellent agreement with the numerical model of Israëls, Leermakers, and Fleer (*Macromolecules* **1994**, *27*, 3249). Simple asymptotic expressions for the rms thickness and the degree of dissociation are also obtained. These approximate relations are found to be in good agreement with both the numerical model and a recent scaling analysis (Zhulina, Birshtein, and Borisov. *Macromolecules* **1995**, *28*, 1491). A pronounced difference between the dependences of the total thickness and rms thickness on the salt concentration is found: the total thickness decreases monotonically as a function of the salt concentration, whereas the rms thickness passes through a maximum. This difference is shown to be due to the quite different shape of the profiles in various regimes of the brush behavior. Simplified approximate expressions are obtained for the position and the height of this maximum in the rms thickness.

Introduction

Polymer brushes[1-8] are very important and interesting both from a theoretical point of view and for practical implementations. They are good models for polymer layers formed upon the adsorption of end-functionalized polymers or block copolymers, for microdomains of block copolymer superstructures, for the corona structure of polymeric micelles, and for some biological brushlike systems.

Charged polymer brushes were studied recently by several groups of investigators.[9-18] Most of these papers were devoted to brushes with a constant number of charges per chain. However, in brushes of weak polyelectrolytes it is unrealistic to fix the number of charges per chain if the brush is in equilibrium with a solution of variable pH (defined as $pH = -\log [H_3O^+]$) and salt concentration. The degree of dissociation is controlled by the pH inside the brush (which generally differs from the bulk pH) and by the dissociation constant of the acid (or basic) groups in the brush. This situation is common for all biological systems and is also relevant in the stabilization of practical systems by polyelectrolytes. Therefore, the modeling of a weak polyacid brush is more important than that of a brush with a fixed charge. So far, only a few papers[16-18] on this theme are available. In ref 16 the analysis is based on the Scheutjens–Fleer model, whereas ref 17 presents a scaling analysis. Some numerical results of a self-consistent-field (SCF) theory based on most-likely trajectories (an approximation that is also used in the present analysis) have been given in ref 18.

These publications[16-18] demonstrated that polymer brushes with weak groups (i.e., with adjustable charges) can exhibit nontrivial behavior which is quite different from that of brushes with fixed charges. In particular, an increase in ionic strength of the solution can lead to electrostatic swelling of a "weak" brush, whereas a brush with fixed charge can only shrink when the salt concentration is increased. This is caused by the effect of salt on the degree of dissociation α of the brush segments. At very low salt concentration, α in a "weak" brush is quite small, and much lower than the degree of dissociation of such groups in the equilibrium bulk solution. Upon addition of salt, α increases toward its bulk solution value. This charging tends to expand the brush, and this tendency may be stronger than the compression effect due to increased screening by salt ions. Similarly, the variation of the grafting density σ can lead to an unusual effect, *viz.* an *in*crease in brush thickness with *de*creasing σ. This can be explained along the same lines: a decreasing grafting density may give a higher degree of dissociation.

The scaling analysis[17] provided scaling laws for this brush behavior, ignoring the details of the internal brush structure. Thus, in this analysis the brush was considered as a homogeneous region with constant volume fraction, polymer charge, and potential. On the other hand, numerical calculations[16,18] focused mainly on this brush structure, taking into account the spatial variation within the brush; however, they could not give analytical dependencies. In this paper we aim to bridge the gap between these two approaches.

We introduce an analytical SCF theory for brushes of a weak polyacid, which leads to an analytical description of both the internal structure of the brush (for which so far only numerical results are available) and of its average characteristics (for which only scaling relations have been derived). In contrast to the numerical models, the present theory provides analytical equations for the thickness of the brush, for the density profile, and for the degree of dissociation of the polyacid as a function of the distance from the surface. Simple asymptotic expressions for the root-mean-square brush thickness are also derived, which are in good agreement with both the numerical model[16] and the scaling analy-

[†] Russian Academy of Science.
[‡] Wageningen Agricultural University.
[⊗] Abstract published in *Advance ACS Abstracts,* April 15, 1995.

0024-9297/95/2228-3562$09.00/0

sis.[17] The advantage of the latter analysis is that not only power laws but also non-power-law dependences and the numerical coefficients are obtained. The present theory is elaborated in a wider range of pH and allows us to analyze the inner structure of the brush, which is impossible in a scaling model.

We start from the SCF formalism as introduced by Semenov[19] and developed later in a number of papers[3-5] for different cases of brush behavior. We extend this treatment to brushes of a weak polyacid. The results will be compared with the numerical theory outlined in ref 16; for a detailed description of this model we refer to the original paper.

General Model

Let us consider a weak polyacid $(HA)_N$ composed of N spherically symmetric units of linear size l. Each polymer chain is attached to an impenetrable surface with dimensionless grafting density σ, immersed in an aqueous electrolyte solution of a given pH. Let the electrolyte be NaCl. Then, we have the following ions in the bulk solution: H_3O^+, OH^-, Na^+, Cl^-. The concentrations of these ions determine the pH and the ionic strength. All these ions, as well as the water molecules, are assumed to be of equal volume l^3, and these species are allowed to penetrate into the brush. For a weak polyacid the degree of dissociation is not fixed, but it is a function of the local pH. The volume fraction of brush charges at distance x from the surface is equal to $\alpha(x)\varphi(x)$, where $\alpha(x)$ is the local degree of ionization of the polyacid and $\varphi(x)$ is the volume fraction of polymer in the brush. Both $\alpha(x)$ and $\varphi(x)$ are, as yet, unknown functions. In this paper we express x, as well as all other length characteristics, in units of l. This facilitates a comparison with the results of a lattice theory.[16]

In order to find the equilibrium distributions of all components, one should analyze the free energy functional of the system. We shall use several assumptions which make this functional simpler. As in ref 17, we assume that the interactions of the mobile ions are dominated by the electrostatics. Then the volume fractions $\varphi_i(x)$ of the ions in the brush are related to those in the bulk solution, Φ_i, through the local electrostatic potential $\psi(x)$ according to Boltzmann's law:

$$\frac{\varphi_i^+(x)}{\Phi_i^+} = e^{-\psi(x)\, e/kT} \equiv y(x) \qquad \frac{\varphi_i^-(x)}{\Phi_i^-} = e^{\psi(x)\, e/kT} \equiv \frac{1}{y(x)} \tag{1}$$

where kT is the thermal energy and e is the elementary charge. The volume fractions of all ions in the brush as well as the electrostatic potential are functions of the distance x from the grafting surface. This makes our analysis different from scaling and allows us to analyze both the detailed inner structure of the brush and average characteristics, such as the mean height, the mean density, and the mean degree of dissociation of the polyacid.

In order to find $\psi(x)$ and the corresponding distributions of ions, one could solve the Poisson–Boltzmann equation. This is done in full in the scheme of ref 16, whereas in ref 18 a Debye–Hückel approximation was employed; both these papers could give only numerical solutions. In this paper we adopt a more simplified approach and use the approximation of local electroneutrality of the brush, which has been shown to be valid in charged brushes when the brush thickness H exceeds by far the characteristic screening length of electrostatic interactions.[15,16] This local electroneutrality concept assumes a complete compensation of the polyelectrolyte charges by the charges of the mobile ions at any height x in the brush. This assumption does not imply that there are no electrostatic interactions; on the contrary, they are assumed to be so strong that no charge separation is allowed. Nor does it mean that the electrostatic potential is zero (or constant): in regions where there is a high polymer charge, there is a large unbalance between mobile cations and anions, so that according to eq 1 ψ is non-zero. The spatial variation $\psi(z)$ is coupled to that of the polymer charge as indicated below (eq 2).

There is a slight inconsistency in the model because $d^2\psi(x)/dx^2$ should be related to the space charge density ϱ according to the Poisson–Boltzmann equation, and we set $\varrho = 0$ from the start. The full numerical computations[16] showed that $d^2\psi(x)/dx^2$ and, consequently, $\varrho(x)$ are quite small. In all cases the difference between the concentration of negative and positive charges is well below 1% of the cation concentration. Hence, a very good approximation for these concentrations and for $\psi(x)$ can be obtained by neglecting this difference. In effect, we abandon the Poisson–Boltzmann equation and replace it by the electroneutrality constraint. This is completely analogous to calculating the equilibrium distributions and the potential in a classical Donnan equilibrium.

The local electrostatic potential can now be expressed as

$$\alpha(x)\varphi(x) = \sum_i \varphi_i^+(x) - \sum_i \varphi_i^-(x) = \Phi^+\left(y(x) - \frac{1}{y(x)}\right) \tag{2}$$

where φ_i^+ refers to i = H_3O^+ or Na^+, φ_i^- refers to i = OH^- or Cl^-, and $\Phi^+ = \Phi_{H_3O^+} + \Phi_{Na^+}$ is the total volume fraction of cations in the bulk solution. In the following we will abbreviate $\Phi_{H_3O^+}$ as Φ_{H^+}. We consider below Φ_{H^+} to be rather small, so that Φ^+ gives in fact the salt concentration (except when no external salt is added).

The free energy can be written as the sum of an elastic term and a mixing term. For the former we use the standard Semenov expression

$$F^{el}(x) = \frac{3\sigma}{2}\int_x^H E(x,y)\, g(y)\, dy \tag{3}$$

where H is the total thickness of the brush, the function $E(x,y)$ determines the local stretching at height x of a chain with its free end located at height y, and $g(y)$ is the distribution function of the free ends. Further details can be found in refs 3–8.

With the above approximations, the local mixing part of the free energy density $f(x)$ (expressed in kT units per volume l^3) is given by the equation:

$$f(x) = \varphi(x)[\alpha(x)\ln\alpha(x) + (1-\alpha(x))\ln(1-\alpha(x)) + \alpha(x)\mu^0_{A^-} + (1-\alpha(x))\mu^0_{HA}] + \sum_i\{\varphi_i(x)[\ln\varphi_i(x) + \mu_i^0]\} \tag{4}$$

where μ_i^0 is the standard chemical potential of a species of type i, which is also expressed in kT units; in the sum also i = H_2O is included. The chemical potentials of A^- and HA define the dissociation constant K_a according to $\log K_a \equiv -pK_A = \mu^0_{HA} - \mu^0_{H^+} - \mu^0_{A^-}$.

The first two terms in eq 4 describe the mixing entropy of charged and uncharged groups. The terms $\varphi_i \ln \varphi_i$ are associated with the translational entropy of the mobile ions as well as the water molecules. The third and fourth terms, where HA corresponds to nondissociated polyacid groups and A^- to dissociated ones, account for the local dissociation equilibrium. We ignore the polyelectrolyte effect; i.e., the charged groups dissociate as if they were isolated in a solution with the local pH. Note that we do not consider any solvency effects; all Flory–Huggins interactions are taken to be zero. Due to the electroneutrality approximation, $f(x)$ does not contain any explicit electrostatic terms, which is allowed because the net charge density is zero in our approximation. Nevertheless, the electrostatic interactions are still accounted for because $\alpha(x)$ is coupled to $y(x)$ through eq 2.

Taking into account this condition of local electroneutrality, eq 2, and the incompressibility condition, $\sum_i \varphi_i(x) + \varphi(x) = 1$, we can evaluate the derivative $\delta f(x)/\delta\alpha(x)$ to give an expression for the local degree of dissociation. From the minimization condition $\delta f(x)/\delta\alpha(x) = 0$ (which is approximate because the elastic free energy in eq 3 does not explicitly depend on $\alpha(x)$ it then follows

$$\frac{\alpha(x)}{1-\alpha(x)} = \frac{K_a}{\Phi_{H^+}}\frac{1}{y(x)} = \frac{\alpha_b}{1-\alpha_b}\frac{1}{y(x)} \tag{5}$$

where α_b is defined by the equation:

$$K_a = \frac{\alpha_b}{1-\alpha_b}\Phi_{H^+} \tag{6}$$

This form of eqs 5 and 6 applies to dilute polymeric systems, where φ_{H_2O} is close to unity. Hence, the results of our analysis are expected to apply for dilute brushes, which is the typical situation when the brush contains charges.

We obtain $\varphi(x)$ as a function of $\alpha(x)$ by eliminating $y(x)$ from eq 5 and substituting the result of eq 2:

$$\varphi(x) = \Phi^+\left(\frac{\alpha_b}{1-\alpha_b}\frac{1-\alpha(x)}{\alpha^2(x)} - \frac{1-\alpha_b}{\alpha_b}\frac{1}{1-\alpha(x)}\right) \tag{7}$$

As shown before (see, e.g., ref 5) the variation of the total free energy with respect to $\varphi(x)$ for brushes of Gaussian elasticity leads to

$$\frac{\delta f(x)}{\delta\varphi(x)} = \Lambda - k^2x^2 \tag{8}$$

with

$$k^2 = 3\pi^2/(8N^2) \tag{9}$$

The constant Λ can be obtained from the boundary conditions $\varphi(H) = 0$ and $\alpha(H) = \alpha_b$, where H is the thickness of the brush. The simplest approach is to ignore the excluded volume effects connected with polymer and mobile ions completely, i.e., to set $\varphi_{H_2O} = 1$. The more general case of polymer and ions with volume ($\varphi_{H_2O} < 1$) is straightforward but gives more complicated equations; this general case is treated in the Appendix. As will be seen in the Results, the simplified version with $\varphi_{H_2O} \approx 1$ is adequate under most conditions. Then differentiation of eq 4 with respect to $\varphi(x)$ gives

$$\ln[1-\alpha(x)] = \Lambda' - k^2x^2 \tag{10}$$

where Λ' and Λ differ only by a constant. With $\alpha(H) = \alpha_b$ an expression for Λ' is obtained:

$$\Lambda' = \ln[1-\alpha_b] + k^2H^2 \tag{11}$$

Combination of eqs 10 and 11 gives

$$\alpha(x) = 1 - (1-\alpha_b)\exp(k^2H^2 - k^2x^2) \tag{12}$$

Equations 12 and 7 give us the dependences of $\alpha(x)$ and $\varphi(x)$ on the external characteristics (i.e., α_b and Φ^+) and on the distance x from the grafting surface. The only remaining problem is that the value of the total thickness H of the brush, defined by the condition $\varphi(H) = 0$, is unknown as yet. In order to obtain H one has to solve the integral equation describing the normalization condition:

$$N\sigma = \int_0^H \varphi(x)\,dx = \Phi^+\left(\frac{\alpha_b}{1-\alpha_b}\int_0^H \frac{1-\alpha(x)}{\alpha^2(x)}\,dx - \frac{1-\alpha_b}{\alpha_b}\int_0^H \frac{1}{1-\alpha(x)}\,dx\right) \tag{13}$$

or, with eq 12:

$$N\sigma = \Phi^+\left(\alpha_b\int_0^H \frac{e^{k^2H^2-k^2x^2}}{(1-(1-\alpha_b)e^{k^2H^2-k^2x^2})^2}\,dx - \frac{e^{-k^2H^2}}{\alpha_b}\int_0^H e^{k^2x^2}\,dx\right) \tag{14}$$

The second integral of eq 14 can be written as $k^{-1}D(kH)$ where $D(\xi)$ is the Dawson integral, defined as

$$D(\xi) = e^{-\xi^2}\int_0^\xi e^{t^2}\,dt \approx \begin{cases} \xi - \frac{2}{3}\xi^3 & \xi \ll 1 \\ \frac{1}{2\xi} & \xi \gg 1 \end{cases} \tag{15}$$

We introduced in eq 15 only the first terms of an analytical expansion for the Dawson integral, which is appropriate in the limiting cases of very low or very high values of ξ (or kH). Unfortunately, we cannot do the same with the first integral in eq 14 without any *a priori* assumptions.

In the next section we will introduce some asymptotic approximations, but we also solved eq 14 numerically to obtain the thickness H of the brush and, from eqs 12 and 7, all the other characteristics of the brush.

In eq 3 we introduced the end-point distribution function $g(x)$. This quantity is directly related to $\varphi(x)$ through $\varphi(x) = (2/\pi)N\sigma\int_x^H g(y)\,(y^2 - x^2)^{-1/2}\,dy$, as has been shown before.[3-5] By an inversion procedure[3-5] $g(x)$ may be obtained explicitly from $\varphi'(x) \equiv d\varphi(x)/dx$, according to $g(x) = -(x/(\sigma N))\int_x^H \varphi'(y)\,(y^2 - x^2)^{-1/2}\,dy$. This result may be verified by substituting the expression for $g(y)$ in $\varphi(x)$, using the standard integral $\int_x^z (y^2 - x^2)^{-1/2}(z^2 - y^2)^{-1/2} y\,dy = \pi/2$. We note that the above equation for $g(x)$ is general for any $\varphi(x)$ and $\varphi'(x)$. In our case $\varphi'(x)$ is obtained by differentiating eq 7 with respect to x (after substituting $\alpha(x)$ from eq 12). The final outcome for $g(x)$ is

$$g(x) = \frac{\Phi^+}{N\sigma} x \int_0^{H^2-x^2} \frac{1}{\sqrt{H^2 - x^2 - t}} \left\{ \alpha_b k^2 e^{k^2 t} \frac{1 + (1-\alpha_b)e^{k^2 t}}{(1-(1-\alpha_b)e^{k^2 t})^3} + \frac{1}{\alpha_b} k^2 e^{-k^2 t} \right\} dt \quad (16)$$

where we have introduced $t \equiv H^2 - y^2$.

Asymptotic Dependences

In this section we derive asymptotic expressions for total thickness H of the brush, defined by $\varphi(H) = 0$, and for the root-mean-square thickness H_{rms}, which is given by

$$H_{rms}^2 = \int_0^H x^2 \varphi(x)\, dx / \int_0^H \varphi(x)\, dx \quad (17)$$

We obtain these asymptotic dependences in the limiting cases of high and low ionic strength, respectively. To that end, we use different assumptions in the two different regimes: the so-called *salted brush* at high salt concentrations and the *osmotic brush* at low salt concentrations.

Salted Brush. This case is easiest to analyze, because the brush characteristics are close to those of a neutral brush with an effective excluded volume which is determined by the electrostatic interactions. Such a salted brush has a parabolic profile, similar to that of a neutral brush. For a parabolic profile, H_{rms} is proportional to H according to the relation $H_{rms} = H/\sqrt{5}$. In this regime $k^2H^2 = (3\pi^2/8)H^2/N^2$ is much smaller than unity.[3-5] Since $(1 - \alpha(x)) < 1$, we can use the expansion

$$\frac{1}{\alpha^2(x)} = \frac{1}{(1-[1-\alpha(x)])^2} = \sum_{n=0}^{\infty} (n+1)(1-\alpha(x))^n$$

which is valid at all values of $\alpha(x)$. In the salted-brush regime $\alpha(x) \approx \alpha_b$ and at $\alpha_b \approx 1$ only a few terms in the expansions are needed. This expansion, together with eq 12, gives for the first integral of eq 13

$$\int_0^H \frac{1-\alpha(x)}{\alpha^2(x)} dx = \sum_{n=0}^{\infty} (n+1)(1-\alpha_b)^{n+1} e^{(n+1)k^2H^2} \int_0^H e^{-(n+1)k^2x^2} dx = \sum_{i=0}^{\infty} a_i (kH)^{2i+1}$$

Note that the last integral is an error function, for which the given series expansion is well-known for $kH \ll 1$, which is the case for a salted brush. The same type of expansion is also valid for the Dawson integral in eqs 13–15. Thus, the result of the expansion of eq 13 is $N\sigma = \sum_{i=0}^{\infty} c_i (kH)^{2i+1}$. The first coefficient c_0 in this series is zero, and the second is $c_1 = (4/3)\Phi^+ k^2 H^3 \alpha_b^{-2}$, where k^2 is defined by eq 9.

When only this second term c_1 is taken into account, eq 13 gives

$$\frac{H^{salt}}{N} \approx \left(\frac{2}{\pi^2} \sigma \frac{\alpha_b^2}{\Phi^+} \right)^{1/3} \quad (18)$$

Since $H_{rms}^{salt} = H^{salt}/\sqrt{5}$, a similar expression applies for H_{rms}^{salt}, with π^2 replaced by $\pi^2 5^{3/2}$.

Osmotic Brush. In the case of low salt concentrations, in the so-called osmotic regime, the entropy of the counterions plays the main role. In this case the degree of ionization $\alpha(x)$ in the brush changes from very low values near the surface to values close to α_b in the outer part of the brush. In order to obtain an asymptotic expression, we assume $\alpha(x)$ to be small in the region $0 < x < H_{rms}$ and to be close to α_b outside this region:

$$\begin{aligned} \alpha(x) &\ll 1 & 0 < x < H_{rms} \\ \alpha_b - \alpha(x) &\ll 1 & H_{rms} < x < H \end{aligned} \quad (19)$$

With these assumptions, the leading term in eq 13 is proportional to $\alpha^{-2}(x)$. In this region $\alpha(x) = 1 - \exp\{\ln(1-\alpha_b) + k^2H^2 - k^2x^2\} \ll 1$. The expansion of the exponent gives

$$\alpha(x) \approx \alpha_0 + k^2x^2 \qquad 0 < x < H_{rms} \quad (20)$$

where α_0 is the degree of dissociation at $x = 0$ and is given by

$$\alpha_0 = -k^2H^2 - \ln(1-\alpha_b) \quad (21)$$

In order to obtain an asymptotic dependence from eq 13, with eq 20 for $\alpha(x)$, we integrate the first term between the limits $x = 0$ and $x = H_{rms}$. The result is $N\sigma = f\varphi^+ k^{-1} \alpha_0^{-3/2} \alpha_b/(1-\alpha_b)$, where the numerical prefactor f is given by $2f = t/(1+t^2) + \text{atan}(t)$, with $t \equiv kH_{rms}/\sqrt{\alpha_0}$. In order to proceed we note that the factor f does not depend strongly on t at $t \geq 1$. To get a reasonable value for H_{rms}^{os}, we make the somewhat arbitrary choice $t \approx 1$ or $\alpha_0 \approx k^2 H_{rms}^2$. In the comparison with the numerical data, below, we will see that this approximation gives excellent agreement. Now the asymptotic dependence is found to be

$$\frac{H_{rms}^{os}}{N} \approx \left(\frac{8}{9} \frac{2+\pi}{\pi^4} \frac{\Phi^+}{\sigma} \frac{\alpha_b}{1-\alpha_b} \right)^{1/3} \quad (22)$$

Equations 18 and 22 give asymptotical relations for the root-mean-square thickness of the brush that are in good agreement with asymptotical dependences obtained in the scaling analysis of ref 17.

A clear advantage of eq 22 is that it gives also the numerical prefactors and that it allows us to obtain an analytical expression for α_0 and, with eq 21, also for H. For α_0 we find

$$\alpha_0 \approx k^2 H_{rms}^2 \approx \left(\frac{1}{\sqrt{6}} \frac{2+\pi}{2\pi} \frac{\Phi^+}{\sigma} \frac{\alpha_b}{1-\alpha_b} \right)^{2/3} \quad (23)$$

Note that, even when the external salt concentration is equal to zero ($\Phi_{Na^+} = 0$), $\Phi^+ = \Phi_{H^+} \neq 0$, so that α_0 is small but not zero. This fact was overlooked in the interpretation of the numerical data in ref 16 and led to a wrong conclusion about neutral brush behavior in the limit of low salt concentrations. For a neutral brush H_{rms} scales as $\sigma^{1/3}$, whereas eq 22 shows $H_{rms} \propto \sigma^{-1/3}$, in agreement with the scaling result.[17] Hence, the $H_{rms}(\sigma)$ trends reverse. A decrease in salt concentration leads ultimately to the case of a brush dissociating in pure water with a mean height as described by eq 22 with $\Phi^+ = \Phi_{H^+}$. Thus, we do not expect to have a fully neutral brush at zero external salt concentration.

The full height of the brush in the osmotic brush regime follows from eq 21:

$$k^2H^2 \approx -\ln(1-\alpha_b) - \alpha_0 \quad (24)$$

where α_0 is given by eq 23.

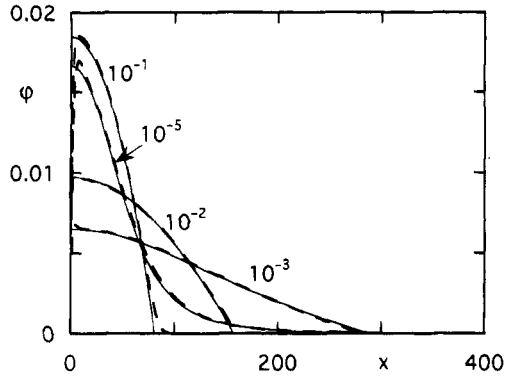

Figure 1. Density profiles $\varphi(x)$ of a polyacid brush at four different volume fractions of salt (indicated). The solid curves were obtained with the analytical theory of the present paper; the dashed curves, with the numerical model of ref 16. Parameters: $N = 500$, $pK_a = 7$, pH = 8, $\sigma = 0.002$.

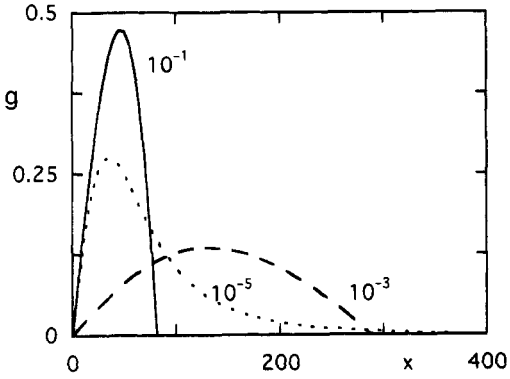

Figure 2. End-point distribution function $g(x)$ of a polyacid brush at three different salt concentrations (indicated). Parameters: as in Figure 1.

Equation 18 shows that H_{rms} and H increase with decreasing salt concentration and increasing grafting density in the salted-brush regime. However, according to eq 22 H_{rms} decreases with decreasing Φ^+ and increasing σ in the osmotic regime, whereas H continues to increase monotonically. At low Φ^+, this increase of H levels off, and the dependences of H on Φ^+ and σ loose their power-law character. At very low salt concentrations H tends to the value $H = [-\ln(1 - \alpha_b)]^{1/2}/k$, which is proportional to N (cf. eq 9) and independent of σ. The rms thickness passes through a maximum at some intermediate salt concentration. The different behavior of H and H_{rms} is a consequence of the rather different shape of the segment density profiles in the two regimes. We return to this point in the following section.

Substitution of eq 24 for k^2H^2 into eqs 20 and 7 gives analytical expressions for the degree of dissociation $\alpha(x)$ and the density profile $\varphi(x)$. For $x = 0$, this results in scaling dependences $\alpha_0 \propto (\Phi^+\alpha_b/\sigma(1 - \alpha_b))^{2/3}$ and $\varphi(0) \propto (\Phi^+\alpha_b/\sigma^4(1 - \alpha_b))^{-1/3}$, which is consistent with the scaling behavior of the mean characteristics $\bar{\alpha}$ and $\bar{\varphi}$ of the brush as a whole, as obtained in ref 17.

Results and Discussion

Figures 1–3 show the segment density profiles, end-point distribution functions and degrees of dissociation of a weak polyacid brush at different salt concentrations. The solid curves in Figures 1 and 3 were computed from eqs 7 and A7, respectively. The more approximate eq 12 instead of eq A7 gives nearly identical results for $\alpha(x)$. However, the values for H, obtained from eq 13 are slightly different. The (rounded) values for H with

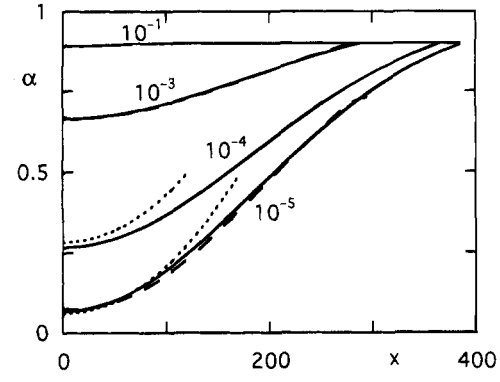

Figure 3. Degree of dissociation $\alpha(x)$ of a polyacid brush at four different salt concentrations (indicated) as a function of the distance to the surface. The solid curves correspond to the analytical theory of the present paper; the dashed curves, to the numerical model of ref 16. The dotted curves were computed from the asymptotic expressions given in eqs 20 and 23. Parameters: as in Figure 1.

eq A7 are 81, 158, 287, 368, and 390 for $\Phi^+ = 10^{-1}$, 10^{-2}, 10^{-3}, 10^{-4}, and 10^{-5}, respectively. The use of eq 12 produces 74, 156, 286, 367, and 389. As a consequence the brush profiles $\varphi(x)$ are slightly more compressed when eq 12 is used, especially when $\varphi(x)$ is relatively high; however, even in those cases the differences are well below 10%. Apparently, excluded volume effects are of minor importance as compared to the electrostatic contributions.

The analytical segment profiles (Figure 1) and the degree of dissociation (Figure 3) are in excellent agreement with those obtained in the numerical calculations;[16] the latter results are given by the dashed curves. In the lattice calculations $l = 0.6$ nm is used and in connection with this the conversion factor from the salt volume fraction to molar salt concentration is 7.7. Except for a narrow depletion zone next to the surface and a "tail" in the periphery of the brush, the analytical and numerical profiles in Figure 1 coincide virtually quantitatively, in the same way as for uncharged brushes.[20] This confirms the validity of using the local electroneutrality approximation instead of the full Poisson–Boltzmann equation.

As already discussed in ref 16, a decrease in the salt concentration from relatively high values (10^{-1}) to rather low values (10^{-5}) results in a nonmonotonical alteration of the profile. At high salt concentrations the profile has a nearly parabolic shape, as for a neutral brush. This is the well-known salted-brush regime, where $\alpha(x)$ is nearly constant ($\alpha(x) \approx \alpha_b$; see Figure 3) because the Coulombic interactions are largely screened by salt ions; the electrostatic interactions can be described through an effective excluded volume which is proportional to the square of $\alpha(x) \approx \alpha_b$ and inversely proportional to $\varphi_+(x) \approx \Phi^+$.[14]

Figure 2 (solid curve) shows the end-point distribution function corresponding to this regime. This also resembles that for a neutral brush.[3,4,19] It is interesting to note that, although the brush almost behaves as a neutral one, its degree of dissociation in this regime is rather high, being nearly equal to that in the bulk solution, α_b; see Figure 3, upper curve.

A decrease in the salt concentration to $\Phi^+ \approx 10^{-2}$–10^{-3} leads to a broadening of the profile and the end-point distribution function. Simultaneously, the thickness H of the brush becomes higher, and the polymer concentration near the surface lower. This decrease is a result of Coulombic repulsion of the polyacid charges,

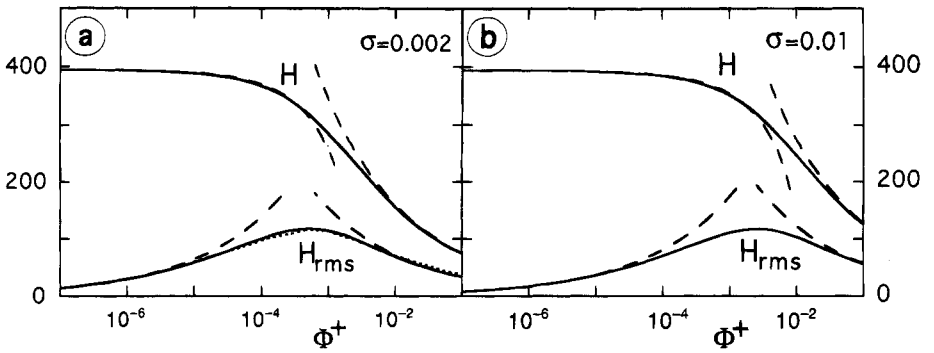

Figure 4. Total thickness H of the polyacid brush and the root-mean-square thickness H_{rms} as a function of salt concentration Φ^+, for two values of grafting density: $\sigma = 0.002$ (a), $\sigma = 0.01$ (b). The solid curves correspond to the analytical theory, and the dashed curves, to the asymptotic dependences given in eqs 18, 22, and 24. The dotted curve for H_{rms} in Figure 4a was calculated with the numerical model of ref 16. Parameters: $N = 500$, $pK_a = 7$, pH = 8.

which is not completely screened at these salt concentrations. From the curve for 10^{-3} in Figure 3 it is clear that the degree of dissociation of the brush molecules is still rather high under these conditions, but the salt concentration is not high enough to screen the repulsion between the charges. As a result, the brush expands. Note that at $\Phi^+ = 10^{-1}-10^{-2}$ (salted brush) $\alpha(x)\,\varphi(x) \ll \Phi^+$, whereas these quantities are nearly equal ($\alpha(x)\,\varphi(x) \approx \Phi^+$) at $\Phi^+ = 10^{-3}$. This concentration corresponds to the transition toward an osmotic brush (where $\alpha(x)\,\varphi(x) \gg \Phi^+$).

Upon further decrease of the salt concentration this expansion does not continue. On the contrary, the internal part of the brush becomes more compact, and the profile in this part resembles that of a near-neutral brush (as for $\Phi^+ = 10^{-1}$). However, the brush profile exhibits a protruding dilute tail. As stated above, in the osmotic regime ($\Phi^+ = 10^{-4}-10^{-5}$) $\alpha(x)\,\varphi(x) \gg \Phi^+$, which can be easily checked from the data given.

As can be seen from the two lower curves in Figure 3, a decrease of Φ^+ down to values $10^{-4}-10^{-5}$ results in a strong decrease of the degree of dissociation of the brush polyacid. The association of the acid groups with protons weakens the Coulombic repulsion and leads to a more compact inner profile. The curve for 10^{-5} in Figure 1 shows that indeed the polymer concentration near the surface is about the same as at $\Phi^+ = 10^{-1}$. Nevertheless, the profile in this case still has a very long tail, which means that the distribution of the free ends in a polyacid brush at low salt concentrations is much wider than that in a neutral brush. This feature is shown clearly in Figure 2 (dotted curve). Since the tail in the profile contributes only slightly to the mean characteristics of the brush, in particular to the rms brush thickness, H_{rms} will be approximately the same in the two limiting cases of high and low salt concentrations. However, the full thickness H of the brush is quite different in these two regimes, being much higher in the limit of the low salt concentration. This could be relevant in, for example, surface-force measurements, where the first interaction is probably determined by H, and not by H_{rms}.

In the case of high salt concentrations (salted brush), where the brush has a parabolic profile, H can be easily estimated from the profile plots. At lower salt concentrations (osmotic brush) the brush is characterized by a quickly decreasing profile at short distances and a slow decay in the periphery. In the latter case H is difficult to define from visual inspection of the profile. However, the mathematical definition on the basis of $\varphi(H) = 0$ is still possible. These values for H were given above.

Figure 4 (upper curves) shows the dependence of the total thickness H of the brush on the salt concentration, for two values of the grafting density: $\sigma = 0.002$ (Figure 4a) and $\sigma = 0.01$ (Figure 4b). These curves were computed from eq 14. Indeed, H is a monotonically decreasing function of Φ^+. The lower solid curves in Figure 4 give the root-mean-square thickness H_{rms}, calculated with eq 17; in Figure 4a also the results for H_{rms} according to the numerical model[16] are given (dotted curve). In contrast to the monotonic variation of H with the salt concentration, H_{rms} shows a maximum at an intermediate ionic strength. The analytical and numerical predictions again virtually coincide. The quite different behavior of $H(\Phi^+)$ and $H_{rms}(\Phi^+)$ might be rather surprising at first sight but is easily explained from the different shapes of the density profiles (compare Figure 1), as discussed above. The maximum in H_{rms} corresponds to the transition between different regimes of brush behavior, from the salted brush to the osmotic brush.[14,16]

The numerical solution for H and H_{rms} in Figures 4a and 4b (solid curves) may be compared with the asymptotic relations for the salted-brush and osmotic-brush regimes as given in eqs 18, 22, and 24. These asymptotes are indicated by the dashed curves in Figure 4a,b. A rather good agreement for the full height of the brush is seen over almost the entire range of the salt concentration; only around the transition salted brush/osmotic brush do deviations occur. The root-mean-square thickness H_{rms} is well described by the approximate dependences only in the two limiting cases of relatively high or low salt concentration. In the intermediate region the asymptotic expressions for H_{rms} deviate considerably from the exact solution because in this region more terms of the expansion should be taken into account. Nevertheless, as will be shown below, the use of these approximations allows us to describe the position of the maximum of H_{rms} on the "numerical" curve, as well as the variation of this maximum as a function of the pH.

Also for conditions other than those shown in Figure 4, the asymptotic dependences of H_{rms} (eqs 18 and 22) describe the trends quite well, both in comparison with the numerical calculations (see ref 16, Figures 5 and 6), and with the scaling predictions.[17] Figure 5 of ref 16 shows the dependence of H_{rms} on σv_{eff}, where $\sigma v_{eff} \approx \sigma\alpha_b^2/\Phi^+$, for the salted-brush regime. The points obtained in the numerical calculations for different sets of the parameters (σ, N, and pH) lie close to the line with a slope $1/3$, in agreement with $H_{rms} \propto (\sigma\alpha_b^2/\Phi^+)^{1/3}$ according to eq 18. Scaling analysis[17] also predicts the same dependence. Figure 6 of ref 16 shows how H_{rms} depends on $\Phi^+K_a/\sigma\Phi_{H^+}$ for the osmotic-brush regime.

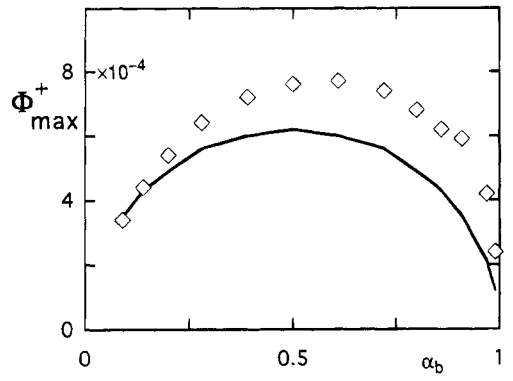

Figure 5. Salt concentration Φ^+_{max} corresponding to the maximum on the curve $H_{rms}(\Phi^+)$ as a function of the degree of dissociation in the bulk solution. The solid curve was calculated with eq 25; the squares are from the numerical model of ref 16. Parameters: $N = 500$, $\sigma = 0.002$.

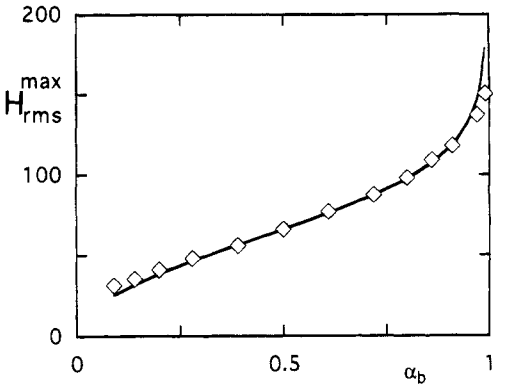

Figure 6. Height of maximum H^{max}_{rms} of the curve $H_{rms}(\Phi^+)$ as a function of the degree of dissociation in the bulk solution. The solid curve was calculated with eq 25 and fixed to the experimental point at $\alpha_b = 0.5$; the squares are from the numerical model of ref 16. Parameters: as in Figure 5.

Since $K_a = \Phi_{H^+}\alpha_b/(1 - \alpha_b)$, the line with a slope $^1/_3$ corresponds to the dependence $H_{rms} \propto (\Phi^+\alpha_b/\sigma(1 - \alpha_b))^{1/3}$, cf. eq 22. The "numerical" points are indeed located close to the line with this slope, although there are some deviations. These deviations are not very surprising: the asymptotic dependences are only valid in the two limiting cases of very high and very low salt concentrations. In the intermediate region the asymptotes can describe only the main trends; no exact agreement may be expected.

In order to analyze the position of the maximum on the curve $H_{rms}(\Phi^+)$, we assume that the position of this maximum is given by the equality of H_{rms} in the salted-brush and the osmotic-brush regimes: $H^{salt}_{rms} = H^{os}_{rms}$. Using the asymptotic expressions even in this range (where according to Figure 4 considerable deviations occur) leads to the result

$$(\Phi^+)_{max} = \frac{3}{2}\frac{1}{5^{3/4}}\frac{\pi}{\sqrt{2+\pi}}\sigma(\alpha_b(1-\alpha_b))^{1/2} \qquad (25)$$

It is interesting to note that there is a nonmonotonic dependence of the maximum position on the pH (or on $\alpha_b = 10^{-pK_a}/(10^{-pK_a} + 10^{-pH})$). Thus, at pH < p$K_a$ ($\alpha_b < 0.5$) an increase in the pH results in a shift of the maximum toward higher values of the salt concentration, but at pH > pK_a ($\alpha_b > 0.5$) the opposite trend is found. Figure 5 shows the dependence of Φ^+_{max} on α_b according to eq 25 (solid curve) and several points obtained from the numerical calculations in ref 16 (indicated by squares). A reasonable qualitative agreement between the theoretical prediction and the numerical results is seen. In both cases, there is a nonmonotonic dependence of Φ^+_{max} on α_b, with a maximum around $\alpha_b = 0.5$. Quantitatively, the agreement is less: the numerical points lie above the theoretical curve. This is due to the rather rough description of the maximum position, which was derived from the equality of two asymptotic relations in a region where these asymptotes are not valid.

Equation 25 illustrates how the maximum in the curve $H_{rms}(\Phi^+)$ shifts with varying coverage σ. In fact, this shift applies to the entire curve and enables us to predict in what region the asymptotical dependences (18) (for the salted brush) and (22) (for the osmotic brush) are valid as σ is varied. For example, in Figure 4a the asymptotic relation for the osmotic brush applies us to about $\Phi^+ \approx 10^{-5}$ at $\sigma = 2 \times 10^{-3}$, whereas in Figure 4b this is the case up to $\Phi^+ \approx 10^{-4}$ at $\sigma = 2 \times 10^{-2}$. This shift is the same as that predicted by eq 25 for the position of the maximum.

We can obtain also the absolute value of H^{max}_{rms} in the same way. Substitution of eq 25 in eq 22 gives

$$\frac{H^{max}_{rms}}{N} = \left(\frac{4}{3}\right)^{1/3}\frac{1}{5^{1/4}}\frac{(2+\pi)^{1/6}}{\pi}\frac{\alpha_b^{1/2}}{(1-\alpha_b)^{1/6}} \qquad (26)$$

Note that H^{max}_{rms} is independent of σ and depends on α_b only. The dependence on α_b is rather strong at high α_b and much weaker ($\propto\alpha_b^{1/2}$) at low α_b. Scaling[17] predicts $H^{max}_{rms} \propto \alpha_b^{1/2}$ for low pH (low α_b), in agreement with eq 26. Figure 6 shows the theoretical dependence $0.5H^{max}_{rms}(\alpha_b)$ (solid curve) and the points H^{max}_{rms} obtained in the numerical calculations[16] (squares). The correction factor 0.5 was chosen such that the analytical curve matched the numerical one at $\alpha_b = 0.5$. As can be seen in Figure 4a,b the intersection of the asymptotic curves gives a much higher value for H^{max}_{rms} than the maximum in the "numerical" curves, because the asymptotes diverge greatly in the intermediate region. With this in mind, a very good semiquantitative agreement is obtained between the approximate eqs 25 and 26 and the numerical data.

From the results of this paper it follows that there are two different measures of the brush thickness, which at small salt contents scale in different ways. The first is the average thickness, defined by some moment of the density distribution. In this paper we considered the second moment H_{rms}; it can be shown, however, that the first and higher moments obey the same scaling rules as H_{rms}. The second measure of the brush thickness is the total size of the brush or the entire width over which the end points of the chains are found.

The analysis of a polyelectrolyte brush with simple scaling considerations[17] provides only one characteristic for the thickness. It is not surprising that this "scaling thickness" is an average property and that the scaling dependences obtained in ref 17 coincide with those obtained for H_{rms} in this paper. The limiting full brush size does not manifest itself at all in the naive scaling picture.

We note that this difference between the average and the limiting brush size for polymeric brushes is found here for the first time. For neutral brushes and for salted brushes, for which the profile has a parabolic shape, the average and maximal brush thicknesses are proportional to each other so that the scaling behavior

is the same. For polyelectrolyte brushes in the osmotic regime the full brush size is related to the contour length of the grafted chains, whereas the density distribution is determined only by the average brush size.

Also the other scaling dependences obtained in ref 17 describe the average brush characteristics. For the degree of dissociation and the brush density these are weight-averaged quantities.

Conclusions

We have analyzed the behavior of a brush of a weak polyacid as a function of the pH and salt concentration in the solution on the basis of analytical SCF theory. We obtained analytical equations for the total thickness and root-mean-square (rms) thickness of the brush, for the density profile, for the end-point distribution function, and for the degree of dissociation of the charge groups in the brush. The analytical results for the segment concentration and the degree of dissociation as a function of the distance from the surface and for the dependence of the rms thickness on the salt concentration are in excellent agreement with the numerical calculations of ref 16. As in this model, we find that the rms thickness passes through a maximum as a function of the salt concentration; however, the total thickness increases monotonically with decreasing ionic strength. We derived also simple asymptotic expressions for the total thickness and rms thickness and for the degree of dissociation in the limiting cases of high and low salt concentrations, corresponding to two different regimes of brush behavior, *viz.* the salted brush and the osmotic brush. These asymptotic dependences are found to be in good agreement both with the numerical model[16] and with a scaling analysis.[17] The advantage of this treatment above both the numerical calculations[16] and the scaling analysis[17] is that it provides analytical equations with all the numerical coefficients for all brush characteristics. The analysis is valid in a wide range of pH and makes it possible to predict rather subtle effects, such as the position and height of the maximum in the rms thickness as a function of the salt concentration.

Acknowledgment. Yu.V.L. acknowledges the hospitality of G.J.F. at Wageningen University and would like also to thank Dr. Ir. P. A. Barneveld for the help with computer programs. E.B.Z. and T.M.B. acknowledge the Russian Foundation for Fundamental Investigations for financial support (Grant 93-03-5797). This work was also partially supported by INTAS.

Appendix. A More Rigorous Equation for $\alpha(x)$

Equations 10–12 were derived under the assumption $\varphi_{H_2O} = 1$. In the more general case $\varphi_{H_2O} \neq 1$, $1 - \alpha(x)$ in eq 10 must be replaced by $(1 - \alpha(x))/\varphi_{H_2O}(x)$, and a similar modification applies to eq 11. Now eq 12 is changed to

$$\alpha(x) = 1 - \frac{\varphi_{H_2O}(x)}{1 - 2\Phi^+}(1 - \alpha_b)e^{k^2H^2 - k^2x^2} \qquad \text{(A1)}$$

where $\varphi_{H_2O}(x)$ equals

$$\varphi_{H_2O}(x) = 1 - 2\Phi^+\frac{1 - \alpha(x)}{\alpha(x)}\frac{\alpha_b}{1 - \alpha_b} - \varphi(x)(1 - \alpha(x)) \qquad \text{(A2)}$$

and $\varphi(x)$ is given by eq 7. Substitution of eq 7 into (A2) and (A2) into (A1) results in a cubic equation in $\alpha(x)$ which may be written as

$$\alpha^3 - p\alpha^2 - q = 0 \qquad \text{(A3)}$$

with

$$p = 1 - (1 - \alpha_b + f/\alpha_b)e^{k^2H^2 - k^2x^2} \qquad \text{(A4)}$$

$$q = f\alpha_b e^{k^2H^2 - k^2x^2} \qquad \text{(A5)}$$

$$f = \frac{\Phi^+}{1 - 2\Phi^+} \qquad \text{(A6)}$$

The solution of (A3) is

$$\alpha(x) = \frac{1}{3}p + (A + B)^{1/3} + (A - B)^{1/3} \qquad \text{(A7)}$$

where

$$A = q/2 + p^3/27 \qquad \text{(A8)}$$

$$B^2 = q(q/4 + p^3/27) \qquad \text{(A9)}$$

From eq A7 $\alpha(x)$ can be directly solved. For $f \to 0$, $\alpha(x) = p$, which is identical to eq 12. Substitution of $\alpha(x)$ as obtained from eq A5 into eqs 7 and 13 provides $\varphi(x)$ and H.

References and Notes

(1) Alexander, S. *J. Phys. (Paris)* **1977**, *38*, 983.
(2) Halperin, A.; Tirrell, M.; Lodge, T. P. *Adv. Polym. Sci.* **1991**, *100*, 31.
(3) Skvortsov, A. M.; Gorbunov, A. A.; Pavlushkov, I. V.; Zhulina, E. B.; Borisov, O. V.; Priamitsyn, V. A. *Polym. Sci. USSR* **1988**, *30*, 1706.
(4) Zhulina, E. B.; Borisov, O. V.; Priamitsyn, V. A. *J. Colloid Interface Sci.* **1990**, *137*, 495.
(5) Zhulina, E. B.; Borisov, O. V.; Priamitsyn, V. A.; Birshtein, T. M. *Macromolecules* **1991**, *24*, 140.
(6) Milner, S. T.; Witten, T. A.; Cates, M. E. *Macromolecules* **1988**, *92*, 6718.
(7) Milner, S. T.; Witten, T. A.; Cates, M. E. *Europhys. Lett.* **1988**, *5*, 413.
(8) Milner, S. T. *Science* **1991**, *251*, 845.
(9) Pincus, P. *Macromolecules* **1991**, *24*, 2912.
(10) Miklavic, S. J.; Marcelja, S. *J. Phys. Chem.* **1988**, *92*, 6718.
(11) Misra, S.; Varanasi, S.; Varanasi, P. P. *Macromolecules* **1989**, *22*, 4173.
(12) Borisov, O. V.; Birshtein, T. M.; Zhulina, E. B. *J. Phys. II, Fr.* **1991**, *1*, 521.
(13) Zhulina, E. B.; Borisov, O. V.; Birshtein, T. M. *J. Phys. II, Fr.* **1992**, *2*, 63.
(14) Borisov, O. V.; Zhulina, E. B.; Birshtein, T. M. *Macromolecules* **1994**, *27*, 4795.
(15) Israëls, R.; Leermakers, F. A. M.; Fleer, G. J.; Zhulina, E. B. *Macromolecules* **1994**, *27*, 3249.
(16) Israëls, R.; Leermakers, F. A. M.; Fleer, G. J. *Macromolecules* **1994**, *27*, 3087.
(17) Zhulina, E. B.; Birshtein, T. M.; Borisov, O. V. *Macromolecules* **1995**, *28*, 1491–1499.
(18) Misra, S.; Varanasi, S. *J. Colloid Interface Sci.* **1991**, *146*, 251.
(19) Semenov, A. N. *Sov. Phys. JETP* **1985**, *61*, 733.
(20) Wijmans, C. M.; Scheutjens, J. M. H. M.; Zhulina, E. B. *Macromolecules* **1992**, *25*, 2657.

MA946137P